Progress In Electromagnetics Research, PIER 88, 227–240, 2008

A SIMPLE ALTERNATIVE FOR BEAM RECONFIGURATION OF ARRAY ANTENNAS

F. Ares

Department of Applied Physics
University of Santiago de Compostela
15782 Santiago de Compostela, Spain

G. Franceschetti †

Department of Electronic Engineering
University of Naples
80125 Napoli, Italy

J. A. Rodriguez

Department of Applied Physics
University of Santiago de Compostela
15782 Santiago de Compostela, Spain

Abstract—An innovative method for antenna arrays beam configuration is presented. In the proposed method, every element of the array is connected to its feed through a switch, so that it can be active or passive, depending on the switch position. Pattern reconfigurability is achieved by appropriately switching on or off the array elements. The optimal configuration of the switches for each of the radiated patterns, as well the common voltages of the active elements, is calculated by using a genetic algorithm. For each configuration, the currents in the driven and parasitic elements are determined, via their self and mutual impedances, by inversion of the impedance matrix. In the presented examples, the method has been applied to both linear and planar arrays of parallel dipoles that switch the power pattern from a pencil to a flat-topped beam (linear array) or to a footprint pattern (planar array).

† Also with University of California, Los Angeles, USA

1. INTRODUCTION

Antenna pattern reconfigurability is considered as a major issue for satellite communications. Satellite operators are willing to optimise the overall capacity of their spacecraft fleet. This requires the capacity of traffic reassignment either just before launch or preferably in flight.

Antenna array pattern reconfiguration is usually achieved by changing the relative amplitudes and/or phases of the excitations of its radiating elements [1–7]. In [8], pattern reconfiguration is obtained using an optimal set of element-perturbed positions. However, these approaches often require the design of beam-forming networks of considerable complexity. A recent work achieved pattern reconfiguration by performing a mechanical displacement of a parasitic array located in front of an active one [9]. The method calculates the currents in the driven and parasitic elements via their self and mutual impedances: their design leads to the desired radiation pattern change, thus achieving the antenna system reconfigurability. However, it has been found that the parasitic array must be very near to the driven array to obtain good results, which may complicate the implementation of the mechanical system that is required to move the parasitic elements. Besides, the method is not useful for applications that require real-time reconfigurability. In [10], parasitic elements were used in the design of a wide scanning phase array antenna.

In this paper we present a method that performs antenna array pattern reconfiguration by appropriately switching on or off the array elements of an array composed of parallel dipoles. A "switched on" element is connected to the feed and performs as a driven element, whereas a "switched off" element is disconnected from the feed and performs as a parasitic element. The required beam-forming network using this method is much simpler than in previous approaches of array pattern reconfiguration.

2. THE ANTENNA ARRAY

Consider a square-meshed array with d inter-element spacing, composed by N $\lambda/2$-dipoles parallel to the z axis and placed on the $y = 0$ plane (Fig. 1). Each dipole is connected to the feed through a switch, so it can be active (with feeding voltage V_n) or passive, as Fig. 2 shows. Modifying the switches configuration changes the configuration (number and location) of driven/parasitic elements: accordingly, the currents of both driven and parasitic dipoles are modified owing to the mutual coupling.

Computation of the radiation diagram requires evaluation of the

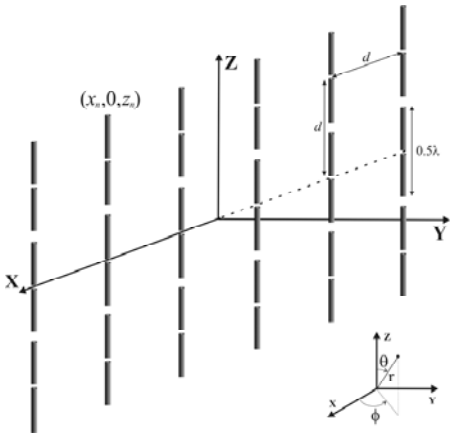

Figure 1. Geometry of the array of dipoles. For reference, a spherical system of coordinates (r, θ, ϕ) is also depicted, for subsequent computation of the radiated field.

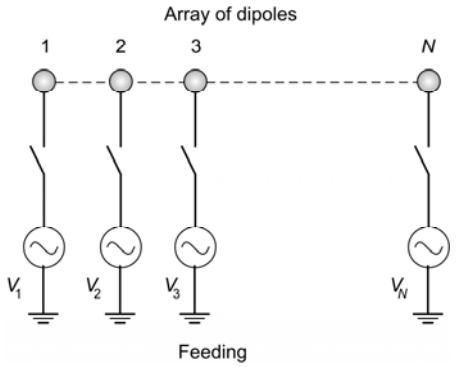

Figure 2. Layout of the switched array.

current distribution. This can be accomplished by using the following matrix equation:

$$[V] = [Z]\,[I] \Rightarrow [I] = [Z]^{-1}\,[V] \tag{1}$$

where $[V]$ is the (known) vector of the complex voltages applied to the driven and parasitic elements (see below), $[I]$ is the (unknown) vector of the relative complex excitations of both the driven and the parasitic elements, and $[Z]$ the impedance matrix. The entries of the latter are calculated by using a commercial software tool based on the

method of moments [11] as far as the self-impedances Z_{nn} of centre-fed cylindrical dipoles are concerned, whereas the mutual impedances Z_{mn} are calculated using analytical expressions. Specifically, the mutual impedance Z_{mn} of two centre-fed dipoles with lengths $2l_m$ and $2l_n$ located at (x_m, y_m, z_m) and (x_n, y_n, z_n) are calculated using the expression given in [12, p. 332] for slender dipoles, when a sinusoidal current distribution is assumed:

$$Z_{mn} = \frac{j30}{\sin kl_m \sin\, kl_n} \int_{-l_n}^{l_n} \left(\frac{e^{-jkr'_1}}{r'_1} + \frac{e^{-jkr'_2}}{r'_2} - 2\cos kl_n \, \frac{e^{-jkr'}}{r'} \right) \sin[k(l_n - |\zeta|)] d\zeta \quad [\text{ohm}] \tag{2}$$

where:

$$r' = \left[(x_m - x_n)^2 + (y_m - y_n)^2 + (z_m - z_n + \zeta)^2\right]^{1/2}$$
$$r'_1 = \left[(x_m - x_n)^2 + (y_m - y_n)^2 + (z_m - z_n + \zeta - l_n)^2\right]^{1/2}$$
$$r'_2 = \left[(x_m - x_n)^2 + (y_m - y_n)^2 + (z_m - z_n + \zeta + l_n)^2\right]^{1/2}$$

The definitions of the variables are given in Fig. 3.

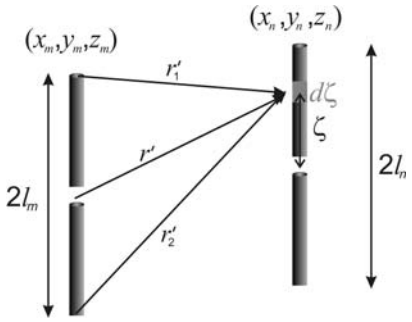

Figure 3. Geometry of two parallel dipoles defining the variables of Equation (2).

It is not worth calculating the mutual impedances by using the method of moments (MoM). As a matter of fact, we found that the values obtained with the expression (2) are quite similar to those obtained by the MoM. Besides, the latter method is not appropriate for its use in a genetic algorithm because it is very slow. Regarding to the self-impedances, since there are only two different dipoles (see next paragraph), they have been previously calculated using [11] and then tabulated on the genetic algorithm.

Since parasitic dipoles are disconnected from the feed, they have no input currents at their gaps. However, if we set $I = 0$ for parasitic dipoles in (1), we are not taking into account their contribution to the radiated pattern. Although the input currents of the parasitic dipoles are zero, the driven elements induce currents along the arms of the parasitic dipoles that do contribute to the radiated pattern of the array. In order to calculate these currents correctly (and thus the radiated pattern), we have modelled every parasitic dipole using the "extra port" method described in [13]. In this method each parasitic dipole is divided into two sub-dipoles (each of length $\lambda/4$) and we define an extra ports at the centre of each sub-dipole. A parasitic dipole with a zero input current is equivalent to two sub-dipoles with a zero voltage at their centres: a null voltage at the extra port yields a maximum current at this point that falls to the edges of each sub-dipoles (see Fig. 4). Accordingly, by setting zero voltages at the extra ports, the current at the centre of the parasitic dipoles becomes negligible. By virtue of the above, the known quantities in the matrix equation (1) are the input voltages applied to the driven elements and the input voltages, equal to zero, of each sub-dipole of the parasitic elements. The unknown quantities are the input currents of the active elements and the induced currents at the centre (input of extra ports) of each sub-dipole. Using the "extra port" method, the number of dipoles to compute is no longer N, but $N + P$, being P the number of parasitic dipoles (switched off), because we have to consider $N - P$ driven $\lambda/2$-dipoles and $2P$ parasitic $\lambda/4$-dipoles.

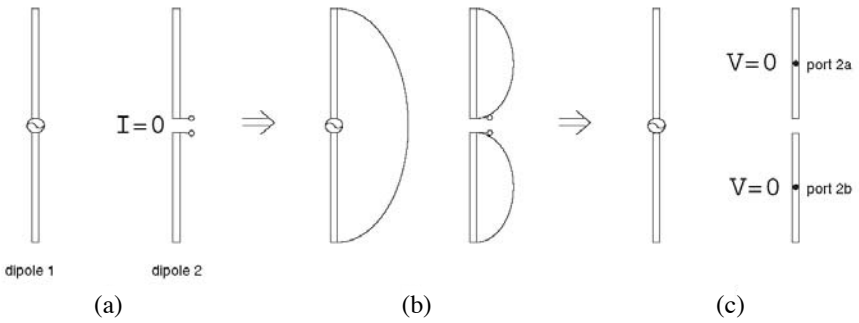

Figure 4. Schematic representation of "extra port" method. (a) Original dipole array: dipole 1, driven element; dipole 2, parasitic element. (b) Current distribution on the dipoles when dipole 1 is excited; (c) Definition of extra ports (dot points) on the parasitic dipole.

The resulting current distribution depends on: i) the configuration of the switches since it determines those dipoles that are performing as driven or parasitic elements; ii) the complex voltages $\{V_1, V_2, \ldots, V_{N-P}\}$ applied to the driven elements. These elements are the design parameters to compute the radiation diagram $F(\theta, \phi)$ of the considered antenna system by following the conventional approach:

$$F(\theta, \phi) = \sum_{m=1}^{N+P} I_m \exp\{jk(x_m \sin\theta\cos\phi + z_m \cos\theta)\} \cdot f_m(\theta) \quad (3)$$

with the m-th driven or parasitic dipole located at $(x_m, 0, z_m)$ and $f_m(\theta)$ being the element factor of dipole m with length $2l_m$ [12]:

$$f_m(\theta) = \frac{-2}{k\sin\theta}\left[\cos(kl_m\cos\theta) - \cos(kl_m)\right] \quad (4)$$

In Equations (3) and (4), because of applying the "extra port" method, $2l_m = \lambda/2$ and $2l_m = \lambda/4$ for driven and parasitic dipoles, respectively. Besides, the centers of parasitic dipoles are vertically displaced $\pm\lambda/8$ from the centers of the driven ones. In the calculation of the radiation pattern, we assumed a sinusoidal distribution of current also on the $\lambda/4$ dipoles, as a result of numerical simulations performed by the MoM [11].

For two prescribed diagrams, a genetic algorithm [14] is used to calculate the optimal configuration of the switches, as well as the complex voltages of the driven elements, to synthesise each pattern. It is noteworthy that the voltages of driven elements are common in both patterns. This method is capable of attaining additional desired features: in the presented example, the minimization of the maximum variation of active impedances of driven elements, $|\Delta\mathrm{Re}(Z_n^A)|_{\max}$ and $|\Delta\mathrm{Im}(Z_n^A)|_{\max}$, when the antenna switches between patterns, is implemented.

When a ground plane is placed behind the array ($y < 0$) to concentrate the radiation toward only one hemisphere of the space, the considerations from the image principle are applied to the self and mutual impedances evaluation. For a ground plane located $\lambda/4$ behind the array, the whole of the above analysis holds if Z_{nn} is replaced by $(Z_{nn} - Z''_{nn})$, where Z''_{nn} is the mutual impedance between the n-th dipole and its image, and Z_{nm} is replaced by $(Z_{nm} - Z''_{nm})$, where Z''_{nm} is the mutual impedance between the n-th dipole and the image of the m-th dipole. The pattern of a dipole plus ground plane, in the half-space $y > 0$, is the pattern of an isolated dipole multiplied by the factor $2j\sin(kh\sin\theta\sin\phi)$ [12]: in this case the expression of the

element factor (4) must be replaced by:

$$f_m(\theta) = \frac{-4j \sin(kh \sin\theta \sin\phi)}{k \sin\theta} \left[\cos\left(kl_m \cos\theta\right) - \cos\left(kl_m\right)\right] \qquad (5)$$

where h is the distance from the dipoles to the ground plane.

The above described method has been validated by using the MoM [11]. Considering small antennas composed by a few driven and parasitic dipoles, we have found that the currents and the patterns obtained by using the proposed method are essentially the same than those obtained by using the MoM.

3. OPTIMIZATION BY USING A GENETIC ALGORITHM

Genetic algorithms are a class of very powerful search methods which are based on stochastic and non deterministic approach and are widely used for non-differentiable function minimizations, that is, for numerical optimization problems in which gradient-based methods are failed. These optimization algorithms have been recently applied to many electromagnetic problems [15–19].

For the purposes of optimization by a genetic algorithm, the design parameters can be described by a chromosome χ made up of $2N + 2$ genes (Fig. 5). The first two genes, each of length N bits, encode the configuration of the N switches of the antenna for each pattern (the value '1' indicates a driven element whereas the value '0' indicates a parasitic one). The additional $2N$ genes, each of length 6 bits, encode the N amplitudes and N phases of the complex voltages applied to driven elements.

The amplitudes $|V_n|$ of the N complex voltages are related to the

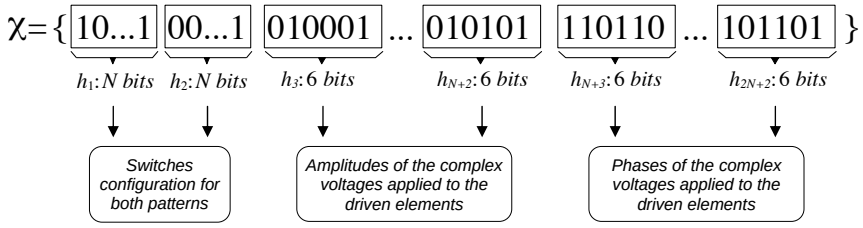

Figure 5. An example of the layout of the $(2N+2)$-gene chromosome describing the configuration of the switches for both patterns and the amplitudes and phases of the complex voltages applied to the driven elements.

bits of the gene by

$$|V_n| = 10^{-a/20}, \quad a = \sum_{q=1}^{6} 2^{q-3} h_{n+2}(q), \quad n = 1, 2, \ldots N \tag{6}$$

where $h_{n+2}(q)$ is the value of the q-th bit of the $(n+2)$-th gene of the chromosome. Each gene thus encodes $|V_n|$ in steps of 0.25 dB in the range $[-15.75,\, 0]$ dB relative to the maximum amplitude.

The phases α_n of the N complex voltages are given in degrees by

$$\alpha_n = 22.5 \times \sum_{q=1}^{6} 2^{q-3} h_{n+N+2}(q), \quad n = 1, 2, \ldots N \tag{7}$$

so that the corresponding gene encodes α_n in steps of 5.625°.

Variations on this scheme can of course be introduced if desired: in the frame of this piece of work, use of a 6-bit code for $|V_n|$ and α_n was convenient for practical reasons related to implementation of beam-forming network using digital commercial attenuators and phase shifters, respectively. Note, however, that using too few bits will mean that the solution space is sampled too coarsely for effective optimizations, and that using too many bits may render the optimization process very slow.

For the examples presented below, where the antenna switches the power pattern from a pencil to a flat-topped beam (linear array) or to a footprint pattern (planar array), optimization is performed to minimize a cost function $C(\chi)$ containing terms controlling the performance of both pencil and flat-topped/footprint beams achieved with a given chromosome χ:

$$C(\chi) = c_1 \Delta_p H(\Delta_p) + c_2 \Delta_{ft} H(\Delta_{ft}) + c_3 \Delta'_{ft} H(\Delta'_{ft}) \tag{8}$$

with:

$$\begin{aligned} \Delta_p &= SLL^{\circ}_p(\chi) - SLL^{d}_p \\ \Delta_{ft} &= SLL^{\circ}_{ft}(\chi) - SLL^{d}_{ft} \\ \Delta'_{ft} &= Ripple^{\circ}_{ft}(\chi) - Ripple^{d}_{ft} \end{aligned}$$

where H is the Heaviside step function that is used to penalize a maximum sidelobe level $SLL^{\circ}(\chi)$ or ripple level $Ripple^{\circ}_{ft}(\chi)$ of the patterns, corresponding to χ, and exceeding the specified tolerable level (SLL^d and $Ripple^d_{ft}$). The subscripts p and ft indicate the pencil beam and the flat-topped/footprint beam, respectively. The coefficients c_i determine the relative weight given to each term. Additional terms

for parameters such as directivity, beamwidth, or variation of active impedances of driven elements when the antenna switches between patterns, could be also included in (8), if desired.

Calculations were performed using a program incorporating SUGAL modules [14]. It was found sufficient to use a population of 300 chromosomes. Population size was constant, with ranked replacement of parents bettered by their offspring. Offspring were generated by one-point crossover and the inclusion of one mutation of every chromosome. The final solution is obtained after 200 generations.

4. NUMERICAL EXAMPLES

4.1. Linear Array

In the first example, we consider a linear array composed by 30 $\lambda/2$-dipoles parallel to the z axis and equispaced $\lambda/2$ along the x axis. A ground plane is located $\lambda/4$ behind the array (at $y = -\lambda/4$, according to the geometry shown in Fig. 1). To reduce the number of variables in the optimisation process, all the design parameters are supposed to be symmetric with respect to the centre of the array.

This antenna will switch its radiation pattern from a pencil to a flat-topped broadside beam by using the switches configurations shown in Table 1 (as previously stated, the value '1' indicates a driven element, whereas the value '0' indicates a parasitic one).

Table 1. Configurations of the switches for pencil and flat-topped beams synthesised by a linear array of 30 $\lambda/2$-dipoles. $N - P$ denotes the number of driven elements in each configuration.

	Pencil beam	*Flat-topped beam*
N-P	28	8
Switches configuration	1111111111101111110111111111111	0000000010010111101001000000000

Figure 6 shows the patterns radiated by this antenna: a with a -18.5 dB sidelobe level and a flat-topped beam pattern with 42 deg. beamwidth measured at -3 dB, ± 0.6 dB of ripple and $SLL = -17.0$ dB. The maximum variation of the active impedance of driven elements obtained in this case is $|\Delta\mathrm{Re}(Z_n^A)|_{\max} = 40.2\,\Omega$ and $|\Delta\mathrm{Im}(Z_n^A)|_{\max} = 47.6\,\Omega$. Since the flat-topped beam is generated by switching off many elements its power is 12.5 dB less than the power of the pencil beam.

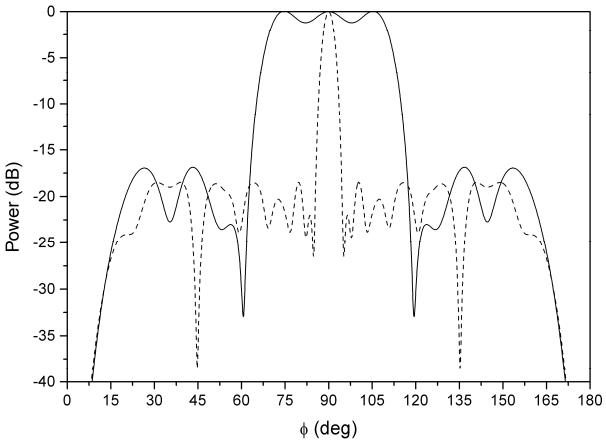

Figure 6. Patterns radiated in the $\theta = \pi/2$ plane by a 30-element linear array of dipoles using the switches configurations of Table 1. Pencil beam; dotted line; Flat-topped beam: solid line. A ground plane is located $\lambda/4$ behind the driven array.

In a new optimization (whose data are not referred in the paper) the maximum variation of the active resistance can be greatly reduced to $|\Delta\mathrm{Re}(Z_n^A)|_{\max} = 14.7\,\Omega$, at the expense of increasing the variation of active reactance $|\Delta\mathrm{Im}(Z_n^A)|_{\max} = 62.5\,\Omega$ and slightly reducing the performance of the patterns (a pencil beam with $-17.3\,\mathrm{dB}$ sidelobe level and a flat-topped beam with $-16.6\,\mathrm{dB}$ sidelobe level and a ripple of $\pm 0.7\,\mathrm{dB}$).

Using the same antenna array, it was possible to switch its radiation pattern from a pencil beam with a $SLL = -20\,\mathrm{dB}$ to a pencil beam with a $SLL = -30\,\mathrm{dB}$ by modifying the state of two switches only.

4.2. Planar Array

In this example we consider a square-meshed array with 0.6λ inter-element spacing composed by 6×6 $\lambda/2$-dipoles parallel to the z axis and placed on the $y = 0$ plane (Fig. 1). As in the previous example, a ground plane is located $\lambda/4$ behind the planar array. To reduce the number of variables in the optimisation process, we used quadrant symmetry in calculation of all the design parameters.

By using the switches configurations shown in Table 2, the antenna will switch its radiation pattern from a pencil beam to a square footprint occupying the region $-0.25 \leq u \leq 0.25,\ -0.25 \leq w \leq 0.25$,

Table 2. Configurations of the switches for pencil and square footprint beams synthesised by a planar array of 6×6 $\lambda/2$-dipoles. $N-P$ denotes the number of driven elements in each configuration.

	Pencil beam	*Square footprint pattern*
N-P	28	20
Switches configuration	110011 111111 011110 011110 111111 110011	001100 001100 111111 111111 001100 001100

where $u = \sin\theta\cos\phi$ and $w = \cos\theta$.

Figure 7 shows the patterns radiated by this antenna: a pencil beam with a $-17.0\,\mathrm{dB}$ sidelobe level and a footprint pattern with $\pm0.4\,\mathrm{dB}$ of ripple in the target square and $SLL = -15.2\,\mathrm{dB}$. The maximum variation of the active impedance of driven elements obtained in this case is $|\Delta\mathrm{Re}(Z_n^A)|_{\max} = 8.9\,\Omega$ and $|\Delta\mathrm{Im}(Z_n^A)|_{\max} = 16.8\,\Omega$. In this case the power of the footprint pattern is $5.9\,\mathrm{dB}$ less than the power of the pencil beam.

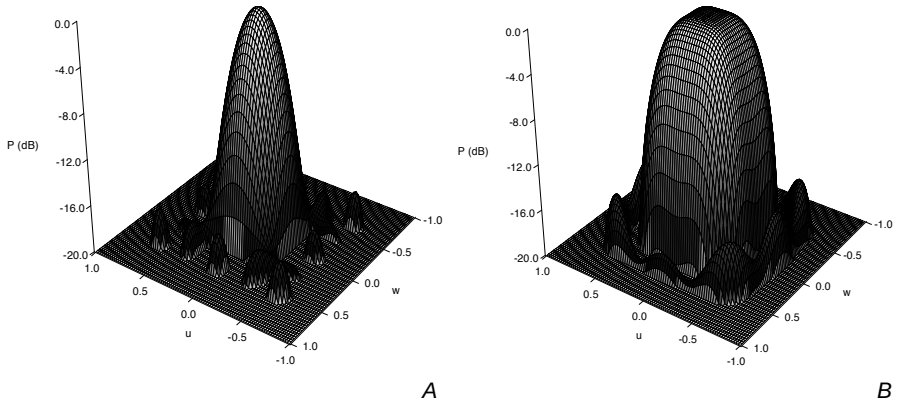

Figure 7. Patterns radiated by a 6×6-element planar array of dipoles using the switches configurations of Table 2. A (left) pencil beam; B (right) footprint pattern occupying the square $-0.25 \le u \le 0.25$, $-0.25 \le w \le 0.25$ ($u = \sin\theta\cos\phi$, $w = \cos\theta$). A ground plane is located $\lambda/4$ behind the driven array.

5. CONCLUSIONS

Presented results show that, by means of a suitable genetic algorithm, beam reconfiguration using an array composed by parallel dipoles can be achieved without requiring the design of complex beamforming networks. The antenna changes its radiated pattern just by modifying the state of some switches that connects the dipoles to its feed. In a practical case, where the use of ON/OFF switches would change the load of the signal path and hence the impedance matching of the antenna array, implementation of SPDT switches would mitigate this issue [20]. The method is useful for applications that require real-time reconfigurability.

In the presented examples, the antenna switches the power pattern from a pencil to a flat-topped beam using a linear array, and from a pencil beam to a square footprint using a planar array. However, the proposed technique may be applied to any other desired radiation pattern reconfiguration.

ACKNOWLEDGMENT

This work has been supported by the Spanish Ministry of Education (MEC) and Science under Project TEC2008-04485.

REFERENCES

1. Bucci, O. M., G. Mazzarella, and G. Panariello, "Reconfigurable arrays by phase-only control," *IEEE Trans. Antennas Propagat.*, Vol. 39, No. 7, 919–925, 1991.
2. Dürr, M., A. Trastoy, and F. Ares, "Multiple pattern linear antenna arrays with single prefixed amplitude distributions: Modified Woodward-Lawson synthesis," *Electron. Lett.*, Vol. 36, No. 16, 1345–1346, 2000.
3. Díaz, X., J. A. Rodríguez, F. Ares, and E. Moreno, "Design of phase-differentiated multiple-pattern antenna arrays," *Microw. Opt. Technol. Lett.*, Vol. 16, No. 1, 52–53, 2000.
4. Brégains, J. C., A. Trastoy, F. Ares, and E. Moreno, "Synthesis of multiple-pattern planar antenna arrays with single prefixed or jointly optimised amplitude distributions," *Microw. Opt. Technol. Lett.*, Vol. 32, No. 1, 74–78, 2002.
5. Trastoy, A., Y. Rahmat-Samii, F. Ares, and E. Moreno, "Two pattern linear array antenna: synthesis and analysis of tolerance,"

IEE Proc. Microw. Antennas Propagat., Vol. 151, No. 2, 127–130, 2004.

6. Mahanti, G. K., A. Chakraborty, and S. Das, "Design of fully digital controlled reconfigurable array antennas with fixed dynamic range ratio," *Journal of Electromagnetic Waves and Applications*, Vol. 21, No. 1, 97–106, 2007.
7. Akdagli, A., K. Guney, and B. Babayigit, "Clonal selection algorithm for design of reconfigurable antenna array with discrete phase shifters," *Journal of Electromagnetic Waves and Applications*, Vol. 21, No. 2, 215–227, 2007.
8. Vaitheeswaran, S. M., "Dual beam synthesis using element position perturbations and the G3-GA algorithm," *Progress In Electromagnetics Research*, PIER 87, 43–61, 2008.
9. Rodríguez, J. A., A. Trastoy, C. Brégains Julio, F. Ares, and G. Franceschetti, "Beam reconfiguration of linear arrays by using parasitic elements," *Electron. Lett.*, Vol. 52, No. 3, 131–133, 2006.
10. Yuan, H. W., S. X. Gong, P. F. Zhang, and X. Wang, "Wide scanning phased array antenna using printed dipole antennas with parasitic element," *Progress In Electromagnetics Research Letters*, Vol. 2, 187–193, 2008.
11. EM Software & Systems-S. A., *FEKO User's Manual Suite 5.1*, EMSS, 2005.
12. Elliott, R. S., *Antenna Theory and Design*, Revised edition, John Wiley and Sons, Inc., Hoboken, New Jersey, 2003.
13. Xi, Y. P., D. G. Fang, Y. X. Sun, and Y. L. Chow, "Mutual coupling in a linear dipole array of finite size," *IEE Proc. Microw. Antennas Propagat.*, Vol. 152, No. 5, 324–330, 2005.
14. Hunter, A., *SUGAL Genetic Algorithm Package v. 2.1*, University of Sunderland, England, 1995.
15. Su, D. Y, D. M. Fu, and D. Yu, Genetic algorithms and method of moments for the design of PIFAs," *Progress In Electromagnetics Research Letters*, Vol. 1, 9–18, 2008.
16. Razavi, S. M. J. and M. Khalaj-Amirhosseini, "Optimization an anechoic chamber with ray-tracing and genetic algorithms," *Progress In Electromagnetics Research B*, Vol. 9, 53–68, 2008.
17. Ngo Nyobe, E., and E. Pemha, "Shape optimization using genetic algorithms and laser beam propagation for the determination of the diffusion coefficient in a hot turbulent jet of air," *Progress In Electromagnetics Research B*, Vol. 4, 211–221, 2008.
18. Liu, B., L. Beghou, and L. Pichon, "Adaptive genetic algorithm based source identification with near-field scanning method,"

Progress In Electromagnetics Research B, Vol. 9, 215–230, 2008.

19. Chen, H. T., G. Q. Zhu, and S. Y. He, "Using genetic algorithm to reduce the radar cross section of three-dimensional anisotropic impedance object," *Progress In Electromagnetics Research B*, Vol. 9, 231–248, 2008.
20. Cheng, D., "Reconfigurable patch antenna apparatus, systems, and methods," Patent application US7403172, July 2008.